Am J Cancer Res 2019;9(8):1734-1745
www.ajcr.us /ISSN:2156-6976/ajcr0097823

*Original Article*

# Wild-type *TP53* defined gamma-secretase inhibitor sensitivity and synergistic activity with doxorubicin in GSCs

Chen Zhang[1], Emmanuel Martinez-Ledesma[1,4], Feng Gao[1], Wei Zhang[1,3], Jie Ding[1], Shaofang Wu[1], Xiaolong Li[1], Jimin Wu[2], Ying Yuan[2], Dimpy Koul[1], WK Alfred Yung[1]

[1]*Department of Neuro-Oncology, Brain Tumor Center, The University of Texas MD Anderson Cancer Center, Houston, TX, USA;* [2]*Department of Biostatistics, The University of Texas MD Anderson Cancer Center, Houston, TX, USA;* [3]*Department of Neurosurgery, Beijing Tiantan Hospital, Capital Medical University, Beijing, China;* [4]*Tecnologico de Monterrey, Escuela de Medicina y Ciencias de la Salud, Monterrey, Nuevo Leon, Mexico*

Received May 31, 2019; Accepted July 15, 2019; Epub August 1, 2019; Published August 15, 2019

**Abstract:** Glioblastoma (GBM) is the most common and lethal primary intracranial tumor. Aggressive surgical resection plus radiotherapy and temozolomide have prolonged patients' median survival to only 14.6 months. Therefore, there is a critical need to develop novel therapeutic strategies for GBM. In this study, we evaluated the effect of NOTCH signaling intervention by gamma-secretase inhibitors (GSIs) on glioma sphere-forming cells (GSCs). GSI sensitivity exhibited remarkable selectivity among wild-type *TP53* (wt-p53) GSCs. GSIs significantly impaired the sphere formation of GSCs harboring wt-p53. We also identified a concurrence between GSI sensitivity, NOTCH1 expression, and wt-p53 activity in GSCs. Through a series of gene editing and drug treatment experiments, we found that wt-p53 did not modulate NOTCH1 pathway, whereas NOTCH1 signaling positively regulated wt-p53 expression and activity in GSCs. Finally, GSIs (targeting NOTCH signaling) synergized with doxorubicin (activating wt-p53) to inhibit proliferation and induce apoptosis in wt-p53 GSCs. Taken together, we identified wt-p53 as a potential marker for GSI sensitivity in GSCs. Combining GSI with doxorubicin synergistically inhibited the proliferation and survival of GSCs harboring wt-p53.

**Keywords:** Glioblastoma, NOTCH signaling, gamma-secretase inhibitor, *TP53*

## Introduction

GBM (World Health Organization grade IV) is the most common and lethal primary intracranial tumor [1]. GBMs exhibit relentless malignant progression, characterized by widespread invasion throughout the brain, resistance to chemical and radiation therapies, and tumor recurrence [2, 3]. Without treatment, most patients die of their disease within 3 months of diagnosis [1]. Surgical intervention can extend survival to 9-10 months, and the addition of adjuvant radiotherapy and temozolomide can lengthen survival to a median of only 14.6 months [1]. Therefore, novel therapeutic strategies are imperative for GBMs.

Identifying relevant biomarkers to predict treatment response has emerged as a promising strategy for GBM treatment. Crizotinib is currently being investigated in *MET*-amplified GBMs (NCT02034981) as part of a larger trial with 23 molecularly defined cohorts [4]. Thus, improved understanding of the molecular pathways driving malignancy will facilitate the development of biomarkers and the evaluation of agents specifically targeting tumor cells, and NOTCH is one of the most urgently wanted pathways under investigation.

NOTCH signaling regulates numerous processes during embryonic and adult development, including neural stem cell biology [5]. Its oncogenic role has been demonstrated in many tumors outside the brain as well as in GBM [6-13]. It has been shown that NOTCH1 expression is significantly upregulated in GBMs [10]. The canonical NOTCH signaling begins when NOTCH ligands bind to the extracellular domain of NOTCH receptors through local cell-cell inter-

actions. When receptors are triggered by ligands, two proteolytic cleavage events are promoted at receptors. NICD, the activated form of NOTCH receptor, relocates to the nucleus, where it interacts with the DNA-binding protein RBPjk, activating a transcriptional complex known as CSL and resulting in the transcription of target genes [14].

Gamma-secretase is an internal protease that cleaves within the membrane-spanning domain of NOTCH receptor to release NICD. GSIs have been widely used in clinical trials targeting NOTCH signaling in many types of tumors [15, 16]. In this study, we observed the concurrence between GSI sensitivity, NOTCH1 expression, and wt-p53 activity in GSCs. We found that NOTCH1 signaling positively regulated wt-p53 activity. The combination of GSI and doxorubicin showed therapeutic benefit in wt-p53 GSCs by inhibiting proliferation and inducing apoptosis.

## Materials and methods

### *Cell lines and reagents*

The GSC lines were established by isolating sphere-forming cells from fresh surgical specimens of human primary GBM tissue, as described previously [17]. Cells were authenticated by testing short tandem repeats using the Applied Biosystems AmpFISTR Identifier kit. The last authentication test was done in July 2018. This study was approved by the institutional review board of The University of Texas MD Anderson Cancer Center (Houston, TX). GSCs were cultured in DMEM/F12 medium containing B27 supplement (Invitrogen, Carlsbad, CA), basic fibroblast growth factor, and epidermal growth factor (20 ng/mL each). The gamma secretase inhibitors RO4929097 and avagacestat were purchased from Selleck Chemicals (Houston, TX), and crenigacestat was provided by Advanced ChemBlocks (Burlingame, CA). Nutlin-3a and doxorubicin were from Sigma-Aldrich (St. Louis, MO). All inhibitors were dissolved in dimethyl sulfoxide.

### *Cell proliferation assay*

The CellTiter-Blue (Promega, Madison, WI) assay was used according to the manufacturer's instructions. GSCs were seeded into 96-well plates at a density of $2 \times 10^3$ cells per well in triplicate. GSIs were added at the indicated concentrations and compared to solvent-treated controls. Doxorubicin concentration for apoptosis detection was determined by IC50 for each GSC. Fluorescence was measured at 570 nm using FLUOstar Omega microplate reader (BMG Labtech, Ortenberg, Germany).

### *Bliss independence model*

The Bliss model was used to compute the expected combined effects of two drugs as the product of their individual effects on the basis of the assumption that there was no drug-drug interaction effect [18-20]. The expected combination effect was calculated using $\text{Effect}_{(a+b)} = E_{(a)} + E_{(b)} - E_{(a)} E_{(b)}$.

The drug combinations were synergistic if their observed effects were higher than the expected combined effects, antagonistic if they were lower, and additive if they were equal. For the GSI and doxorubicin combination analysis, data were included when the level of doxorubicin-induced inhibition was statistically significant but no more than 95% of the untreated value. The difference between the observed and expected Bliss outcome at every dose was calculated accordingly.

### *Sphere formation assay*

GSCs were seeded in 96-well plates (1 cell/well) by flow cytometry sorting and treated with GSIs (1 μM RO, avagacestat, or crenigacestat). GSC293 and GSC236 were treated for 8 weeks. GSC16, GSC34, GSC240, GSC7-10, GSC3-28, and GSC8-18 were treated for 6 weeks. Other GSCs were treated for 4 weeks. The treatment time for each cell line was determined by their doubling time. The number of wells with sphere formation were counted and recorded using the Cell3 iMager CC-5000 System (SCREEN Holdings, Kyoto, Japan).

For GSC34, flowcytometry sorting was introduced to generate single cell-derived subclones in order to detect NOTCH1 and wt-p53 expression. The single cell-derived spheres generated under RO treatment were defined as the RO-resistant (RO-R) subclones. Two subclones were randomly selected and expanded in a 6-well plate under 1 μM RO treatment. The resistance was confirmed using a sphere formation assay, which demonstrated that RO-R subclones had similar sphere formation abilities, with or without GSI treatment.

*Western blot analysis*

Cells were harvested in lysis buffer, as described previously, and subjected to Western blot analysis [21]. As pLIX-hN1ICD plasmid encoded the NICD1 protein sequence from 1770-2555 amino acids, it could not be detected by anti-NICD1 antibody, which detects the cleavage between 1753 and 1754 amino acids. Thus, we used anti-NOTCH1 antibody, which detected epitopes between 2400 and 2500 amino acids, to blot the exogenous NICD1 overexpression. The detailed antibody information is listed in Table S1.

*Quantitative PCR (qPCR)*

Total RNA was extracted from GSCs with an RNeasy Mini kit (Qiagen, Hilden, Germany), according to the manufacturer's instructions. Real-time qPCR was performed with the SuperScript III One-Step RT-PCR System and SYBR Green PCR Master Mix (Invitrogen), according to the manufacturer's instructions. The primers (Sigma-Aldrich, St. Louis, MO) for quantitative PCR are *NOTCH1*-F: TGGACCAGATTGGGGAGTTC, *NOTCH1*-R: GCACACTCGTCTGTGTTGAC, *HES1*-F: CCTGTCATCCCCGTCTACAC, *HES1*-R: CACATGGAGTCCGCCGTAA, *HES5*-F: AAGCACAGCAAAGCCTTCGT, *HES5*-R: CTGCAGGCACCACGAGTAG, *P21*-F: TGGAGACTCTCAGGGTCGAAA, *P21*-R: GGCGTTTGGAGTGGTAGAAATC, *BAX*-F: CCCGAGAGGTCTTTTTCCGAG, and *BAX*-R: CCAGCCCATGATGGTTCTGAT.

*Flow cytometry*

For the cell cycle analysis, disassociated GSCs were stained using a PI/RNase staining buffer according to the manufacturer's instructions (BD Biosciences, Franklin Lakes, NJ). For apoptosis detection, $1 \times 10^6$ cells were collected and resuspended in 100 μL of binding buffer. FITC annexin V (5 μL) and 7-amino-actinomycin D (7-AAD) (5 μL) were added and mixed. Cells were incubated for 15 minutes in dark at ambient temperature. Samples were tested using BD FACSCelesta (BD Biosciences, Franklin Lakes, NJ) and analyzed using FlowJo software version 10.3.

*Transfection and viral infection*

For the CRISPR-Cas9-mediated p53 knockout, p53 double nickase plasmid (sc-416469-NIC, Santa Cruz Biotechnology, Dallas, TX) and control double nickase plasmid (sc-437281, Santa Cruz Biotechnology) were transfected into GSC23 with Lipofectamine 2000 (Invitrogen) for 48 hours. Cells with green fluorescent proteins were sorted by flow cytometry and plated onto 96-well plates to form single colonies. After 6 weeks, the single cell-derived colonies were collected, and p53 expression was detected by Western blot analysis to select p53 knockout subclones.

pLenti6/V5-p53_wtp53 was a gift from Bernard Futscher (Addgene plasmid #22945) [22]. pLIX_403 was a gift from David Root (Addgene plasmid #41395). pLIX-hN1ICD was a gift from Julien Sage (Addgene plasmid #91897) [23]. Lentiviruses were generated using 293FT packaging cells and the VSV-G and PAX2 plasmids. Forty-eight hours after infection, cells were selected by the addition of 5 μg/mL blasticidin or 1 μg/mL puromycin (Invitrogen). Doxycycline (2 μg/ml) was used to induce NICD1 expression in pLIX-hN1ICD-infected cells.

*Statistical analysis*

Statistical analyses were performed using SAS 9.4 (SAS Institute Inc., Cary, NC, USA) and GraphPad Prism software 8.0.0 (GraphPad Software, San Diego, CA, USA). D'Agostino-Pearson test is used to determine if a data set is well-modeled by a normal distribution. F-test is used to test if the variances of two populations are equal. Whether two sets of data were significantly different was determined by unpaired two-tailed Student t-tests (for data sets with normal distribution and equal variance), Welch's t-test (for data sets with normal distribution and unequal variances), or Wilcoxon rank-sum test (for data sets without normal distribution). The mean values shown represent the mean of at least three independent experiments, and the error bars represent the standard deviations.

## Results

*GSI-sensitive GSCs harbored elevated NOTCH1 signaling as well as Wt-p53 activity*

Using the single-cell sphere formation assay, we tested the sensitivity of a panel of GSCs to RO4929097 (RO), a potent and selective GSI. RO significantly abrogated sphere formation in three of 10 GSCs in the screening group ($P < 0.05$) (**Figure 1A**). Consistent with the results of

a previous report, GSI-sensitive GSCs harbored elevated NOTCH1, NICD1, and HES1 expression [17] (**Figure 1B**, **1C**). Notably, all the GSI-sensitive GSCs were wt-p53 lines, while all the GSI-resistant GSCs were mutant *TP53* (mut-p53) lines. GSI-sensitive GSCs also exhibited significantly higher wt-p53 activity than did GSI-resistant GSCs, as shown by the upregulated expression of p21 and BAX (p53 target genes) ($P < 0.05$) (**Figure 1B**, **1C**).

To validate our finding that wt-p53 GSCs were sensitive to GSI, we introduced two more GSIs (avagacestat and crenigacestat) and tested the sensitivity of another set of cell lines (validation group) consisting of five wt-p53 and two mut-p53 GSCs. GSCs showed consistent responses to RO, avagacestat (ava), and crenigacestat (cre) at the same dose. As expected, GSIs significantly impaired sphere formation in four of the five wt-p53 GSCs ($P < 0.01$), while both mut-p53 lines were resistant to GSIs (**Figures 1D**, S1 and S2).

Taken together with these two data sets, we tested 17 GSCs and identified seven GSI-sensitive GSCs, all of which harbored wt-p53 and significantly upregulated p21 and BAX expression ($P < 0.01$) (**Figure 2A-C**). All nine mut-p53 GSCs were resistant to GSIs. Wt-p53 GSCs were more sensitive to GSIs than were mut-p53 GSCs ($P < 0.01$), although GSC3-28 was the only cell line that harbored wt-p53 and was resistant to GSIs. Furthermore, NOTCH1 expression was significantly upregulated in wt-p53 GSCs ($P < 0.01$) (**Figure 2D**).

Our data showed the concurrence between GSI sensitivity, NOTCH1 expression, and wt-p53 activity. Although GSIs downregulated the expression of stem cell markers in wt-p53 and mut-p53 GSCs (Figure S3), GSIs inhibited sphere formation of wt-p53 GSCs only. Our previous study has demonstrated a reasonable role for NOTCH1 activity in predicting GSI responses in GSCs [17], here, we further identified that wt-p53 with NOTCH1 activity was equally efficient in predicting GSI response, suggesting that wt-p53 is a potential marker for GSI sensitivity in GSCs.

*Wt-p53 signaling did not regulate NOTCH1 activity*

Given the significant correlation between NOTCH1 and wt-p53 activity, we studied the underlying mechanism of this concurrence. To determine whether wt-p53 regulates NOTCH1 signaling, we transformed p53 in GSC23 (mut-p53, GSI-resistant) by knocking out the innate mutant p53 and introducing wt-p53. To minimize off-target effects of CRISPR-Cas9-mediated knockout (KO), we randomly selected two single cell-derived mut-p53-KO subclones in this experiment [24, 25]. We also introduced wt-p53 in GSC293 (wt-p53, GSI-sensitive) in parallel. However, wt-p53 overexpression did not affect NOTCH1 activity in either GSC23 mut-p53-KO subclones or GSC293 (wt-p53) (**Figure 3A**). The expression levels of NOTCH1, NICD, and HES1 did not change. We further showed that treating wt-p53 cells with Nutlin-3, a specific MDM2 inhibitor that restores wt-p53 expression, did not influence NOTCH1 activity in wt-p53 GSCs (**Figure 3B**), indicating that wt-p53 does not regulate NOTCH1 activity in GSCs.

*NOTCH1 signaling positively regulated Wt-p53 activity*

Next, we tested if NOTCH1 signaling altered wt-p53 activity, and we tested that by overexpressing NICD1 or RO-induced NOTCH1 downregulation in GSCs. Overexpression of NICD1 in GSC293 (wt-p53) increased p53 and p21 expression levels, indicating that upregulating NOTCH1 activates wt-p53 (**Figure 4A**). We validated this finding by showing that downregulation of NOTCH1 suppressed wt-p53. We isolated two single cell-derived RO-resistant (RO-R) subclones from GSC34 (wt-p53, GSI-sensitive) as described in Materials and Methods section. The resistance was confirmed by decreased sphere formation in all three GSIs-treated GSC subclones (**Figure 4B**). Notably, RO-R subclones harbored significantly decreased NOTCH1 expression and activity (as reflected by NICD1 and HES1 expression levels), as well as attenuated wt-p53 activity (as reflected by p53, p21, and BAX expression levels) ($P < 0.01$), while all single cell-derived subclones from parental GSC34 harbored comparable wt-53 activity, suggesting that the resistance is acquired rather than from subclonal selection and that downregulation of NOTCH1 signaling inhibits wt-p53 activity (**Figures 4C**, **4D**, and S4). Together, these results support that NOTCH1 signaling positively regulates wt-p53 expression and activity in GSCs.

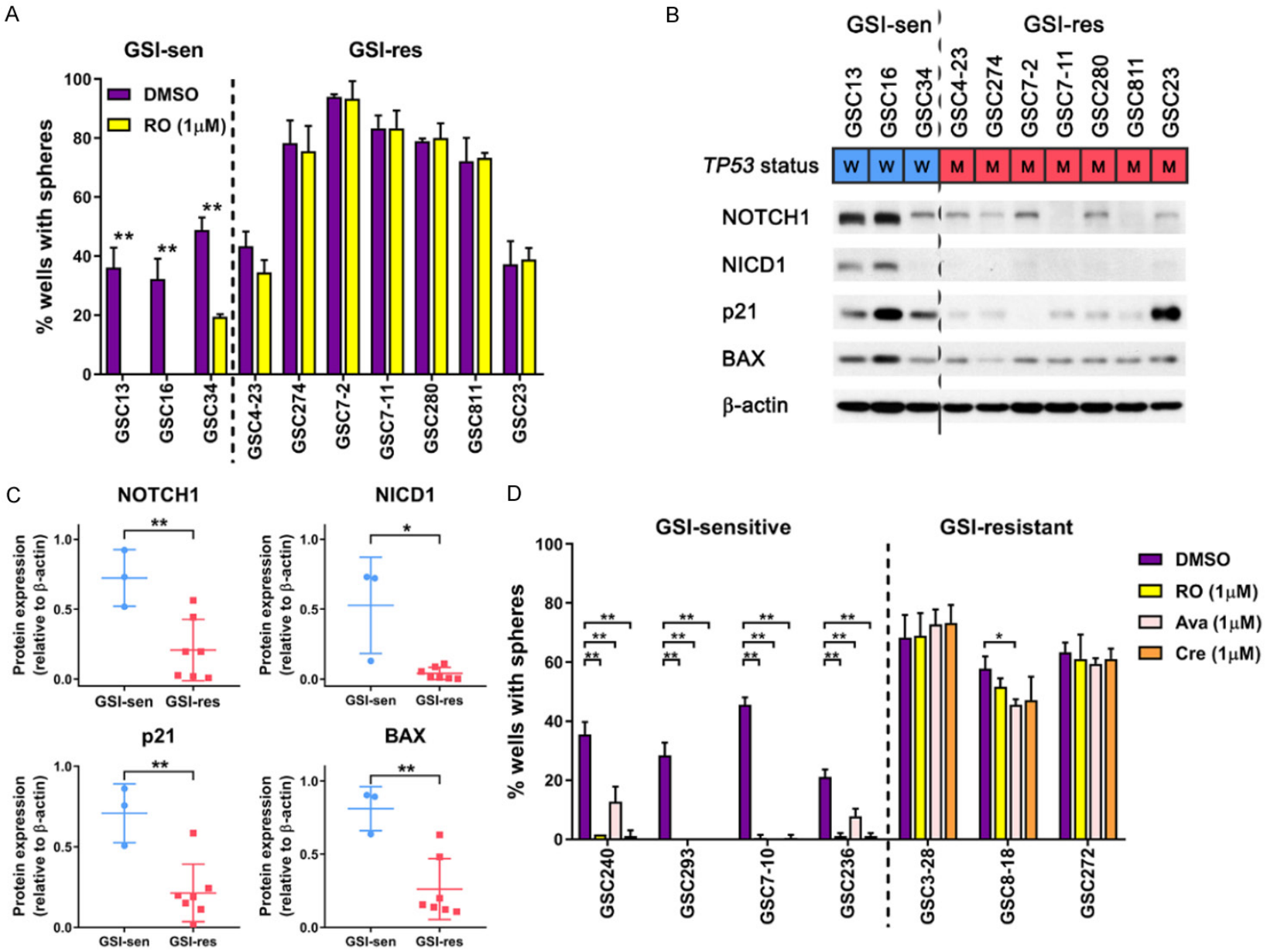
A
GSI-sen
GSI-res
DMSO
RO (1μM)
% wells with spheres
GSC13
GSC16
GSC34
GSC4-23
GSC274
GSC7-2
GSC7-11
GSC280
GSC811
GSC23
B
GSI-sen
GSI-res
TP53 status
W
M
NOTCH1
NICD1
p21
BAX
β-actin
C
NOTCH1
NICD1
p21
BAX
Protein expression (relative to β-actin)
GSI-sen
GSI-res
D
GSI-sensitive
GSI-resistant
DMSO
RO (1μM)
Ava (1μM)
Cre (1μM)
% wells with spheres
GSC240
GSC293
GSC7-10
GSC236
GSC3-28
GSC8-18
GSC272

**Figure 1.** Identification of GSI-sensitive GSCs. A. Three RO-sensitive and seven RO-resistant GSCs were identified using sphere formation assay. B, C. The basal expression of NOTCH1 signaling (NOTCH1 and NICD1) and p53 target genes (p21 and BAX) was detected by Western blot analysis. D. GSCs' sensitivity to three GSIs (RO, avagacestat, and crenigacestat) were tested, and four GSI-sensitive GSCs were identified using sphere formation assay. *TP53* status (W: wild-type, M: mutant) is also shown. Data are represented as means ± SD. *: P < 0.05. **: P < 0.01. n = 3.

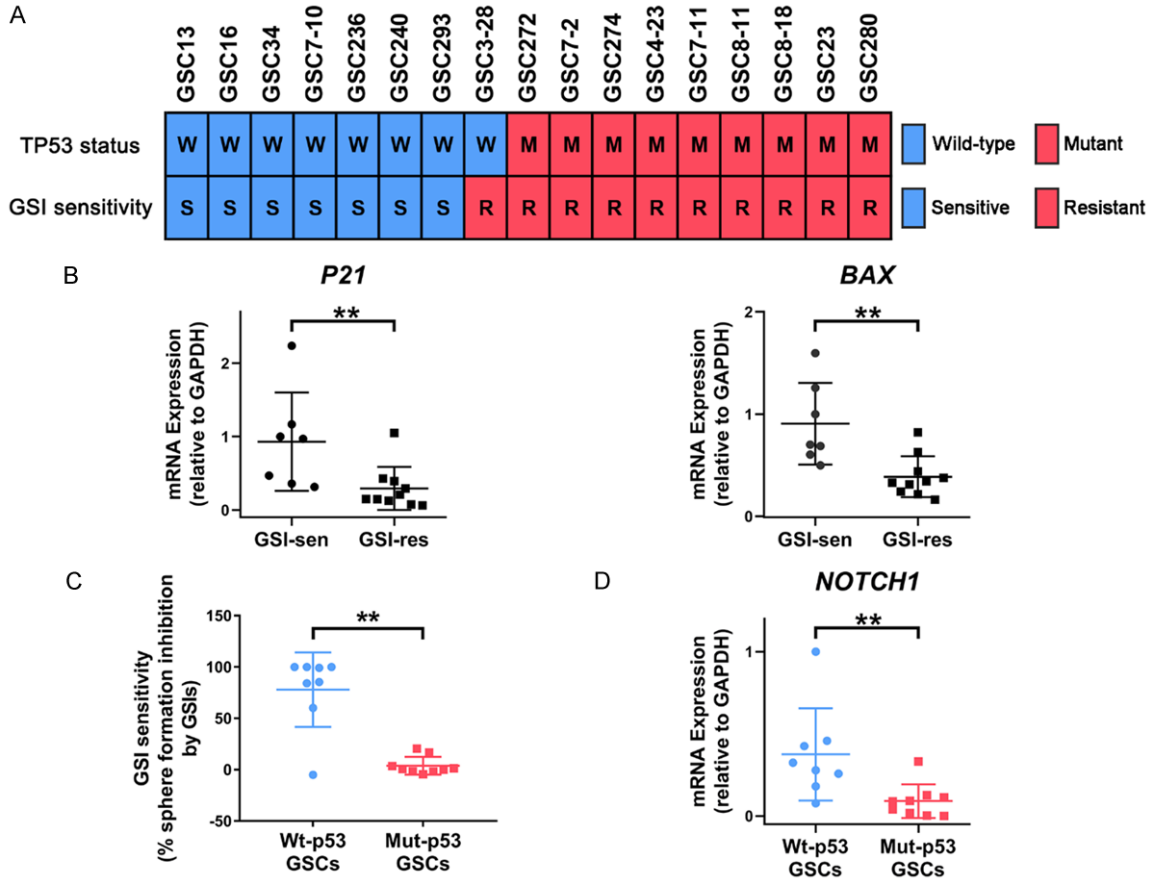


**Figure 2.** Summary of GSI sensitivity signature. A. Seven of eight wt-p53 GSCs were GSI sensitive, while all mut-p53 GSCs were GSI resistant. B. GSI-sensitive GSCs harbored significantly higher p53 target genes (*P21* and *BAX*) expression than GSI-resistant GSCs. C. GSIs inhibited the sphere formation ability of GSCs harboring wt-p53 instead of mut-p53. D. Wt-p53 GSCs harbored significantly higher NOTCH1 expression than mut-p53 GSCs. Data are represented as means ± SD. **: P < 0.01. n = 3.

*GSIs synergized with doxorubicin to inhibit proliferation and induce apoptosis in Wt-p53 GSCs*

Next, our focus was to identify a combination strategy to strengthen GSIs' effect (Figure S5). Given the concurrence of wt-p53 and NOTCH1 in GSI-sensitive GSCs, we sought to determine whether activating wt-p53 augmented GSIs' effect. For that, we introduced doxorubicin, a widely used chemotherapeutic agent that activates wt-p53 [26-28]. GSCs in the screening group were treated with RO/Ava + doxorubicin. GSCs in the validation group were treated with RO/Ava/Cre + doxorubicin. The combination effect was evaluated using the Bliss independency model [18-20]. The combination of GSI and doxorubicin showed more significant anti-proliferative effect in wt-p53 GSCs than in mut-p53 GSCs, as shown by substantial synergistic inhibition of proliferation in wt-p53 GSCs in comparison to mut-p53 GSCs (P < 0.001) (**Figures 5A**, **5B**, S6 and S7). Notably, all three GSIs (RO, Ava, and Cre) had a comparable growth inhibition effect in combination with doxorubicin, indicating a generalized effect of GSIs

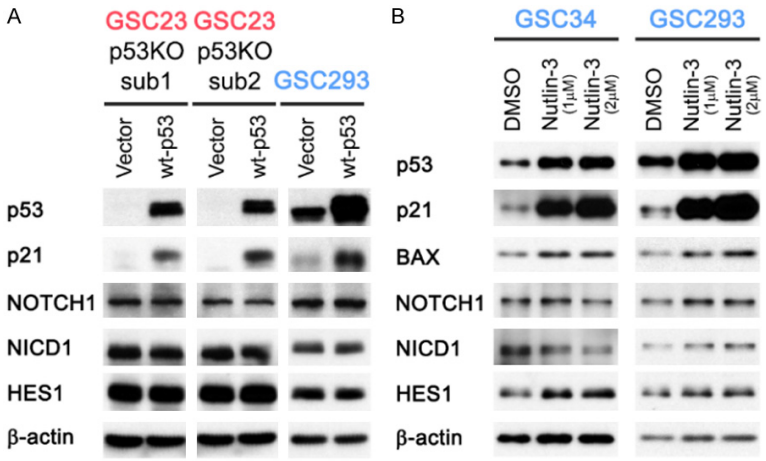


**Figure 3.** Wt-p53 did not regulate NOTCH1 signaling in GSCs. A. *TP53* mutant was knocked out (KO) from GSC23. Then Wt-p53 was introduced into two p53KO subclones. Wt-p53 was also introduced into GSC293, which harbored innate wt-p53. The expression of p53 and NOTCH1 pathway components was detected by Western blot analysis. B. The expression of p53 and NOTCH1 pathway components was detected after Nutlin-3 treatment (24 hours) in two wt-p53 GSCs (GSC34 and GSC293) by Western blot analysis. n = 3. Blue font: wt-p53 cells. Red font: mut-p53 cells.

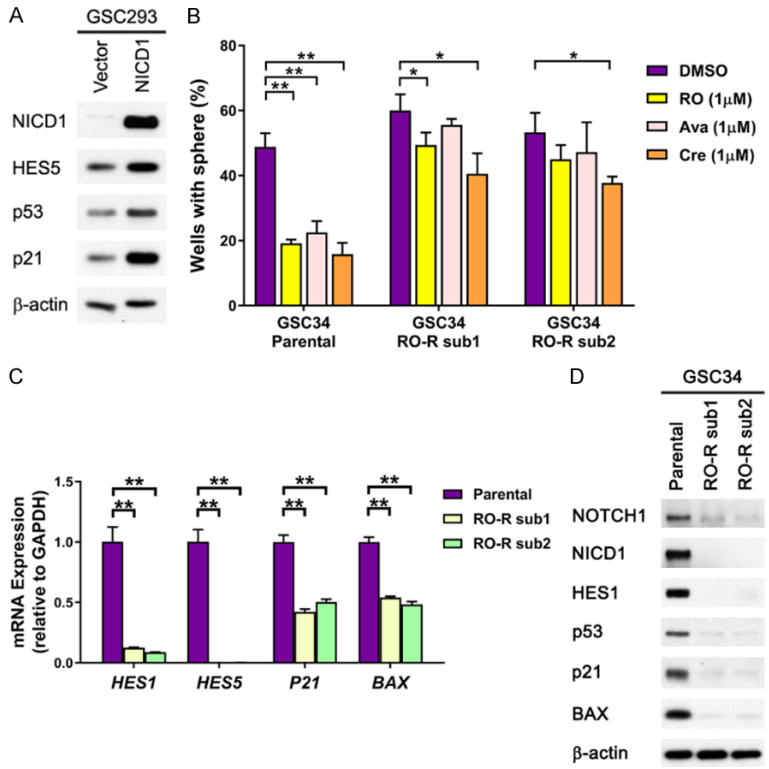


**Figure 4.** NOTCH1 signaling positively regulated wt-p53 activity in GSCs. A. Introducing NICD1 in GSC293 (wt-p53) upregulated p53 and p21 expression. GSCs were treated with doxycycline (2 μg/mL) for 96 hours. B-D. RO-R subclones were derived from GSC34 (wt-p53). B. Both RO-R subclones showed resistance to avagacestat and crenigacestat compared with parental GSC34, as demonstrated using the sphere formation assay. C. The expression of NOTCH1 target genes (*HES1* and *HES5*) and p53 target genes (*P21* and *BAX*) in RO-R subclones was detected by qPCR. D. The expression of NOTCH1 and p53 pathway components in RO-R subclones was detected by Western blot analysis. Data are represented as means ± SD. *: P < 0.05. **: P < 0.01. n = 3. Blue font: wt-p53 cells. Red font: mut-p53 cells.

that is not limited to any one specific GSI.

We further studied the effect of combination treatment of GSI and doxorubicin on cell cycle arrest. GSI plus doxorubicin did not induce additional cell cycle arrest, although doxorubicin alone induced G2/M arrest in all of the GSCs tested [29] (Figure S8). However, GSI plus doxorubicin induced more apoptosis in wt-p53 lines than in mut-p53 lines, as shown by increased number of annexin V-stained cells (**Figures 5C**, **5D** and S9). Increased caspase-3 cleavage and PARP1 cleavage was also induced by combined treatment in wt-p53 GSCs but not in mut-p53 GSCs (**Figures 5E** and S10).

## Discussion

In our study, we showed that wt-p53 GSCs were sensitive to GSI treatment, and NOTCH signaling upregulated wt-p53 expression and activity. Combining GSI and doxorubicin synergistically inhibited proliferation and induced apoptosis in GSCs with wt-p53. Wt-p53 served as a marker for GSI sensitivity as well as for the synergistic activity.

Gamma-secretase was originally identified as the protease responsible for the generation of amyloid β peptides (Aβ), Gamma-secretase cleaves APP within its transmembrane domain and generates multiple Aβ peptides. and thus

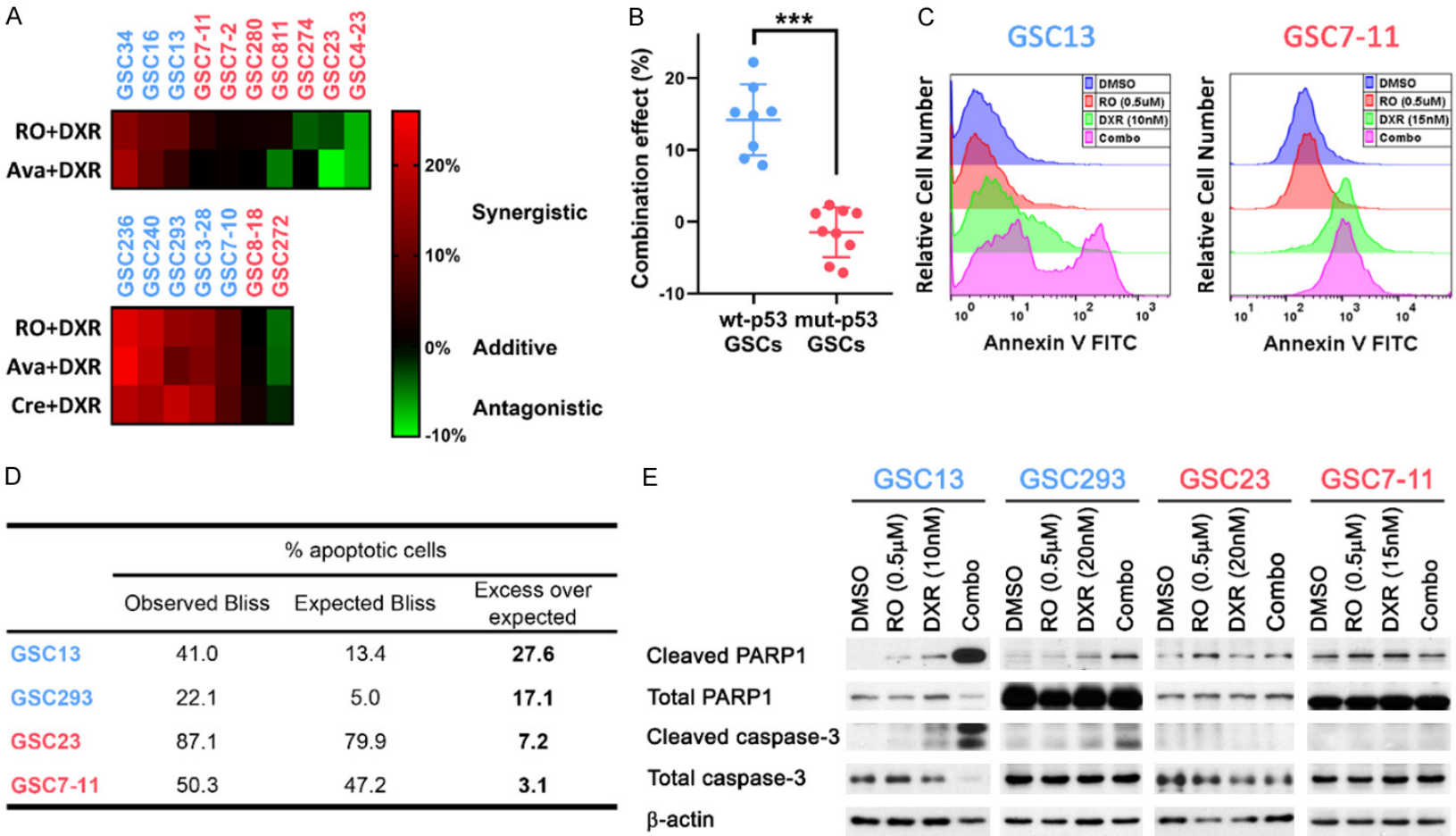


| | % apoptotic cells | | |
|---|---|---|---|
| | Observed Bliss | Expected Bliss | Excess over expected |
| GSC13 | 41.0 | 13.4 | **27.6** |
| GSC293 | 22.1 | 5.0 | **17.1** |
| GSC23 | 87.1 | 79.9 | **7.2** |
| GSC7-11 | 50.3 | 47.2 | **3.1** |

**Figure 5.** Doxorubicin synergistically augmented cytotoxicity of GSIs in wt-p53 GSCs. A. GSCs were treated with the combination of GSI and doxorubicin (DXR) for 5 days. The combination effect was analyzed using the Bliss independency model. GSI plus DXR exerted the more apparent synergistic effect in wt-p53 GSCs than in mut-p53 GSCs. B. Combining GSI with DXR exerted more significantly synergistic anti-proliferative effect in wt-p53 GSCs than in mut-p53 GSCs. Each point represents the average combination effect by GSIs and DXR treatment for each cell line. C, D. RO- and DXR-induced apoptosis was tested by flow cytometry. The combination effect was analyzed using the Bliss independency model. RO plus DXR induced more apoptosis in wt-p53 GSCs than in mut-p53 GSCs. See also Figure S5. E. RO- and DXR-induced apoptosis was detected by PARP1 and caspase-3 cleavage levels. RO plus DXR induced PARP1 and caspase-3 cleavage in wt-p53 GSCs. See also Figure S6. Doxorubicin concentration for apoptosis detection was determined by IC50 for each GSC. ***: $P < 0.001$. n = 3. Blue font: wt-p53 cells. Red font: mut-p53 cells.

serves as a prime therapeutic target in Alzheimer's disease (AD) [30]. Amyloid β protein precursor (APP) and NOTCH are the two major substrates of gamma-secretase. It has been shown that APP promotes tumor cell proliferation, while Aβ inhibits tumor cell proliferation [31-34]. GSIs treatment would increase APP level and decrease Aβ level, and the total effect would be promoting tumor cell growth. Thus, we believe that GSI-induced anti-tumoral effects result from the impaired NOTCH activation rather than APP cleavage. APP would be a potential candidate responsible for GSI resistance in GBMs, which deserves future study.

*TP53* is subject to inactivation by mutation or deletion in > 29% of primary GBMs, according to The Cancer Genome Atlas database. In this study, we found that wt-p53 GSCs harbored elevated NOTCH1 signaling and were sensitive to GSIs. Wt-p53 is a marker for the synergistic activity of GSIs, when administered in combination with doxorubicin. Our study suggests that the combinational treatment of GSIs with doxorubicin would benefit GBM cases harboring wt-p53, providing personalized therapeutic strategy for this group of patients. In this study, the impaired tumorigenicity of wt-p53 GSCs made it difficult to validate these findings in vivo, which was reflected by the decreased self-renewal abilities of wt-p53 GSCs compared with those of mut-p53 GSCs. Wt-p53 GSCs exhibited low tumorigenicity for intracranial xenografts in nude mice (data not shown), and this phenomenon has been supported by the results of the current studies. The loss of p53 function is associated with increased tumorigenicity in lymphoma cells [35]. Meletis et al. have shown that p53 negatively regulated the self-renewal of neural stem cells [36]. As similar molecular mechanisms may control proliferation and brain tumor initiation in GSCs and neural stem cells [37], it is reasonable to speculate that wt-p53 cells harbor the lower self-renewal ability than do mut-p53 cells in GBM.

To further explore the correlation between NOTCH1 and p53, we performed a series of gene-editing experiments in GSCs. We found that NOTCH1 signaling positively regulated wt-p53 activity, while wt-p53 signaling did not regulate NOTCH1 activity. Other studies have indicated that p53 positively regulates NOTCH signaling, but it is important to note that NOTCH signaling and p53 activity interaction can be context dependent [38]. In primary human keratinocytes, p53 positively regulated NOTCH signaling by binding to the NOTCH1 promoter [39-41]. Similarly, NOTCH1 promoter served as a direct p53 binding target in HCT116 colon carcinoma cells [42]. However, NOTCH signaling positively regulated p53 in GBM in our study, as well as in several published articles. Purow et al. showed that silencing NOTCH1 decreased wt-p53 expression and activity in U87-MG cells [43]. Overexpressing NICD2 in CD133+ GBM cells upregulated p53 expression [44]. Furthermore, NOTCH1-induced increases in p53 expression and activity have been observed in human hepatocellular carcinoma [45], in oral carcinoma [46], and during early neural development [47].

Taken together, our findings indicate that GSI sensitivity exhibits remarkable selectivity among wt-p53 GSCs. NOTCH1 signaling positively regulated wt-p53 activity. Wt-p53 could be used as a potential marker for GSI sensitivity, and GSIs synergized with doxorubicin to inhibit proliferation and survival of wt-p53 GSCs.

## Acknowledgements

This study was funded by a National Brain Tumor Society (Defeat GBM) Grant, National Foundation for Cancer Research (NFCR) to W. K. A. Yung, a SPORE grant (P50 CA127001 to F. F. Lang), and a Cancer Center Support Grant (CA016672). The authors thank Ann Sutton in Scientific Publications department for manuscript editing.

## Disclosure of conflict of interest

W.K. Alfred Yung discloses a conflict of interest as a consultant with DNATrix. The rest of the authors have no conflicts of interest to disclose.

**Address correspondence to:** WK Alfred Yung and Dimpy Koul, Department of Neuro-Oncology, Unit 1002, The University of Texas MD Anderson Cancer Center, 1515 Holcombe Blvd., Houston, TX 77030, USA. Tel: 713-794-1285; Fax: 713-794-4999; E-mail: wyung@mdanderson.org (WAY); Tel: 713-834-6202; Fax: 713-834-6230; E-mail: dkoul@mdanderson.org (DK)

## References

[1] Gilbert MR, Dignam JJ, Armstrong TS, Wefel JS, Blumenthal DT, Vogelbaum MA, Colman H,

Chakravarti A, Pugh S, Won M, Jeraj R, Brown PD, Jaeckle KA, Schiff D, Stieber VW, Brachman DG, Werner-Wasik M, Tremont-Lukats IW, Sulman EP, Aldape KD, Curran WJ Jr and Mehta MP. A randomized trial of bevacizumab for newly diagnosed glioblastoma. N Engl J Med 2014; 370: 699-708.

[2] Zhao K, Wang L, Li T, Zhu M, Zhang C, Chen L, Zhao P, Zhou H, Yu S and Yang X. The role of miR-451 in the switching between proliferation and migration in malignant glioma cells: AMPK signaling, mTOR modulation and Rac1 activation required. Int J Oncol 2017; 50: 1989-1999.

[3] Zhu M, Chen L, Zhao P, Zhou H, Zhang C, Yu S, Lin Y and Yang X. Store-operated Ca(2+) entry regulates glioma cell migration and invasion via modulation of Pyk2 phosphorylation. J Exp Clin Cancer Res 2014; 33: 98.

[4] Touat M, Idbaih A, Sanson M and Ligon KL. Glioblastoma targeted therapy: updated approaches from recent biological insights. Ann Oncol 2017; 28: 1457-1472.

[5] Aguirre A, Rubio ME and Gallo V. Notch and EGFR pathway interaction regulates neural stem cell number and self-renewal. Nature 2010; 467: 323-327.

[6] Fan X, Matsui W, Khaki L, Stearns D, Chun J, Li YM and Eberhart CG. Notch pathway inhibition depletes stem-like cells and blocks engraftment in embryonal brain tumors. Cancer Res 2006; 66: 7445-7452.

[7] Fan X, Khaki L, Zhu TS, Soules ME, Talsma CE, Gul N, Koh C, Zhang J, Li YM, Maciaczyk J, Nikkhah G, Dimeco F, Piccirillo S, Vescovi AL and Eberhart CG. NOTCH pathway blockade depletes CD133-positive glioblastoma cells and inhibits growth of tumor neurospheres and xenografts. Stem Cells 2010; 28: 5-16.

[8] Zhu TS, Costello MA, Talsma CE, Flack CG, Crowley JG, Hamm LL, He X, Hervey-Jumper SL, Heth JA, Muraszko KM, DiMeco F, Vescovi AL and Fan X. Endothelial cells create a stem cell niche in glioblastoma by providing NOTCH ligands that nurture self-renewal of cancer stem-like cells. Cancer Res 2011; 71: 6061-6072.

[9] Zhang C, Hai L, Zhu M, Yu S, Li T, Lin Y, Liu B, Zhou X, Chen L, Zhao P, Zhou H, Huang Y, Zhang K, Ren B and Yang X. Actin cytoskeleton regulator Arp2/3 complex is required for DLL1 activating Notch1 signaling to maintain the stem cell phenotype of glioma initiating cells. Oncotarget 2017; 8: 33353-33364.

[10] Hai L, Zhang C, Li T, Zhou X, Liu B, Li S, Zhu M, Lin Y, Yu S, Zhang K, Ren B, Ming H, Huang Y, Chen L, Zhao P, Zhou H, Jiang T and Yang X. Notch1 is a prognostic factor that is distinctly activated in the classical and proneural subtype of glioblastoma and that promotes glioma cell survival via the NF-kappaB(p65) pathway. Cell Death Dis 2018; 9: 158.

[11] Purow B. Notch inhibition as a promising new approach to cancer therapy. Adv Exp Med Biol 2012; 727: 305-319.

[12] Ma Y, Cheng Z, Liu J, Torre-Healy L, Lathia JD, Nakano I, Guo Y, Thompson RC, Freeman ML and Wang J. Inhibition of farnesyltransferase potentiates NOTCH-targeted therapy against glioblastoma stem cells. Stem Cell Rep 2017; 9: 1948-1960.

[13] Xie Q, Wu Q, Kim L, Miller TE, Liau BB, Mack SC, Yang K, Factor DC, Fang X, Huang Z, Zhou W, Alazem K, Wang X, Bernstein BE, Bao S and Rich JN. RBPJ maintains brain tumor-initiating cells through CDK9-mediated transcriptional elongation. J Clin Invest 2016; 126: 2757-2772.

[14] Hori K, Sen A and Artavanis-Tsakonas S. Notch signaling at a glance. J Cell Sci 2013; 126: 2135-2140.

[15] Olsauskas-Kuprys R, Zlobin A and Osipo C. Gamma secretase inhibitors of notch signaling. Onco Targets Ther 2013; 6: 943-955.

[16] Andersson ER and Lendahl U. Therapeutic modulation of notch signalling--are we there yet? Nat Rev Drug Discov 2014; 13: 357-378.

[17] Saito N, Fu J, Zheng S, Yao J, Wang S, Liu DD, Yuan Y, Sulman EP, Lang FF, Colman H, Verhaak RG, Yung WK and Koul D. A high Notch pathway activation predicts response to gamma secretase inhibitors in proneural subtype of glioma tumor-initiating cells. Stem Cells 2014; 32: 301-312.

[18] Zhao W, Sachsenmeier K, Zhang L, Sult E, Hollingsworth RE and Yang H. A new bliss independence model to analyze drug combination data. J Biomol Screen 2014; 19: 817-821.

[19] Wright C, Iyer AKV, Kaushik V and Azad N. Antitumorigenic potential of a novel Orlistat-AICAR combination in prostate cancer cells. J Cell Biochem 2017; 118: 3834-3845.

[20] Gautam P, Karhinen L, Szwajda A, Jha SK, Yadav B, Aittokallio T and Wennerberg K. Identification of selective cytotoxic and synthetic lethal drug responses in triple negative breast cancer cells. Mol Cancer 2016; 15: 34.

[21] Wu S, Wang S, Gao F, Li L, Zheng S, Yung WKA and Koul D. Activation of WEE1 confers resistance to PI3K inhibition in glioblastoma. Neuro Oncol 2018; 20: 78-91.

[22] Junk DJ, Vrba L, Watts GS, Oshiro MM, Martinez JD and Futscher BW. Different mutant/wild-type p53 combinations cause a spectrum of increased invasive potential in nonmalignant immortalized human mammary epithelial cells. Neoplasia 2008; 10: 450-461.

[23] Lim JS, Ibaseta A, Fischer MM, Cancilla B, O'Young G, Cristea S, Luca VC, Yang D, Jahchan NS, Hamard C, Antoine M, Wislez M, Kong C,

Cain J, Liu YW, Kapoun AM, Garcia KC, Hoey T, Murriel CL and Sage J. Intratumoural heterogeneity generated by notch signalling promotes small-cell lung cancer. Nature 2017; 545: 360-364.

[24] Wang Q, Hu B, Hu X, Kim H, Squatrito M, Scarpace L, deCarvalho AC, Lyu S, Li P, Li Y, Barthel F, Cho HJ, Lin YH, Satani N, Martinez-Ledesma E, Zheng S, Chang E, Sauve CG, Olar A, Lan ZD, Finocchiaro G, Phillips JJ, Berger MS, Gabrusiewicz KR, Wang G, Eskilsson E, Hu J, Mikkelsen T, DePinho RA, Muller F, Heimberger AB, Sulman EP, Nam DH and Verhaak RGW. Tumor evolution of glioma-intrinsic gene expression subtypes associates with immunological changes in the microenvironment. Cancer Cell 2017; 32: 42-56, e6.

[25] Kimberland ML, Hou W, Alfonso-Pecchio A, Wilson S, Rao Y, Zhang S and Lu Q. Strategies for controlling CRISPR/Cas9 off-target effects and biological variations in mammalian genome editing experiments. J Biotechnol 2018; 284: 91-101.

[26] Sun Y, Xia P, Zhang H, Liu B and Shi Y. P53 is required for Doxorubicin-induced apoptosis via the TGF-beta signaling pathway in osteosarcoma-derived cells. Am J Cancer Res 2016; 6: 114-125.

[27] Wang S, Konorev EA, Kotamraju S, Joseph J, Kalivendi S and Kalyanaraman B. Doxorubicin induces apoptosis in normal and tumor cells via distinctly different mechanisms. intermediacy of H(2)O(2)- and p53-dependent pathways. J Biol Chem 2004; 279: 25535-25543.

[28] Dunkern TR, Wedemeyer I, Baumgartner M, Fritz G and Kaina B. Resistance of p53 knockout cells to doxorubicin is related to reduced formation of DNA strand breaks rather than impaired apoptotic signaling. DNA Repair (Amst) 2003; 2: 49-60.

[29] Tyagi AK, Singh RP, Agarwal C, Chan DC and Agarwal R. Silibinin strongly synergizes human prostate carcinoma DU145 cells to doxorubicin-induced growth Inhibition, G2-M arrest, and apoptosis. Clin Cancer Res 2002; 8: 3512-3519.

[30] Golde TE, Koo EH, Felsenstein KM, Osborne BA and Miele L. Gamma-secretase inhibitors and modulators. Biochim Biophys Acta 2013; 1828: 2898-2907.

[31] Lim S, Yoo BK, Kim HS, Gilmore HL, Lee Y, Lee HP, Kim SJ, Letterio J and Lee HG. Amyloid-beta precursor protein promotes cell proliferation and motility of advanced breast cancer. BMC Cancer 2014; 14: 928.

[32] Tsang JYS, Lee MA, Ni YB, Chan SK, Cheung SY, Chan WW, Lau KF and Tse GMK. Amyloid precursor protein is associated with aggressive behavior in nonluminal breast cancers. Oncologist 2018; 23: 1273-1281.

[33] Zhao H, Zhu J, Cui K, Xu X, O'Brien M, Wong KK, Kesari S, Xia W and Wong ST. Bioluminescence imaging reveals inhibition of tumor cell proliferation by Alzheimer's amyloid beta protein. Cancer Cell Int 2009; 9: 15.

[34] Brothers HM, Gosztyla ML and Robinson SR. The physiological roles of amyloid-beta peptide hint at new ways to treat Alzheimer's disease. Front Aging Neurosci 2018; 10: 118.

[35] Cherney BW, Bhatia KG, Sgadari C, Gutierrez MI, Mostowski H, Pike SE, Gupta G, Magrath IT and Tosato G. Role of the p53 tumor suppressor gene in the tumorigenicity of Burkitt's lymphoma cells. Cancer Res 1997; 57: 2508-2515.

[36] Meletis K, Wirta V, Hede SM, Nister M, Lundeberg J and Frisen J. p53 suppresses the self-renewal of adult neural stem cells. Development 2006; 133: 363-369.

[37] Singh SK, Hawkins C, Clarke ID, Squire JA, Bayani J, Hide T, Henkelman RM, Cusimano MD and Dirks PB. Identification of human brain tumour initiating cells. Nature 2004; 432: 396-401.

[38] Dotto GP. Crosstalk of notch with p53 and p63 in cancer growth control. Nat Rev Cancer 2009; 9: 587-595.

[39] Lefort K, Mandinova A, Ostano P, Kolev V, Calpini V, Kolfschoten I, Devgan V, Lieb J, Raffoul W, Hohl D, Neel V, Garlick J, Chiorino G and Dotto GP. Notch1 is a p53 target gene involved in human keratinocyte tumor suppression through negative regulation of ROCK1/2 and MRCKalpha kinases. Genes Dev 2007; 21: 562-577.

[40] Mandinova A, Lefort K, Tommasi di Vignano A, Stonely W, Ostano P, Chiorino G, Iwaki H, Nakanishi J and Dotto GP. The FoxO3a gene is a key negative target of canonical notch signalling in the keratinocyte UVB response. EMBO J 2008; 27: 1243-1254.

[41] Yugawa T, Handa K, Narisawa-Saito M, Ohno S, Fujita M and Kiyono T. Regulation of Notch1 gene expression by p53 in epithelial cells. Mol Cell Biol 2007; 27: 3732-3742.

[42] Roemer K. Notch and the p53 clan of transcription factors. Adv Exp Med Biol 2012; 727: 223-240.

[43] Purow BW, Sundaresan TK, Burdick MJ, Kefas BA, Comeau LD, Hawkinson MP, Su Q, Kotliarov Y, Lee J, Zhang W and Fine HA. Notch-1 regulates transcription of the epidermal growth factor receptor through p53. Carcinogenesis 2008; 29: 918-925.

[44] Wang J, Wakeman TP, Lathia JD, Hjelmeland AB, Wang XF, White RR, Rich JN and Sullenger BA. Notch promotes radioresistance of glioma stem cells. Stem Cells 2010; 28: 17-28.

[45] Qi R, An H, Yu Y, Zhang M, Liu S, Xu H, Guo Z, Cheng T and Cao X. Notch1 signaling inhibits growth of human hepatocellular carcinoma through induction of cell cycle arrest and apoptosis. Cancer Res 2003; 63: 8323-8329.

[46] Duan L, Yao J, Wu X and Fan M. Growth suppression induced by Notch1 activation involves Wnt-beta-catenin down-regulation in human tongue carcinoma cells. Biol Cell 2006; 98: 479-490.

[47] Yang X, Klein R, Tian X, Cheng HT, Kopan R and Shen J. Notch activation induces apoptosis in neural progenitor cells through a p53-dependent pathway. Dev Biol 2004; 269: 81-94.

**Table S1.** Primary antibodies information

| Target | Manufacturer | Species | Dilution factor |
|---|---|---|---|
| NOTCH1 | Cell signaling #4380 | Rabbit | 1000 |
| NICD1 | Cell signaling #4147 | Rabbit | 1000 |
| HES1 | Cell signaling #11988 | Rabbit | 10000 |
| HES5 | Abcam #194111 | Rabbit | 10000 |
| p53 | BD Pharmingen #554293 | Mouse | 1000 |
| p21 | BD Pharmingen #556430 | Mouse | 1000 |
| BAX | Cell signaling #5023 | Rabbit | 1000 |
| NESTIN | Millipore #MAB5326 | Mouse | 1000 |
| CD133 | Abcam #16518 | Rabbit | 1000 |
| PARP1 | SCBT #7150 | Rabbit | 500 |
| Cleaved PARP1 | Cell signaling #5625 | Rabbit | 1000 |
| Cleaved caspase-3 | Cell signaling #9661 | Rabbit | 1000 |

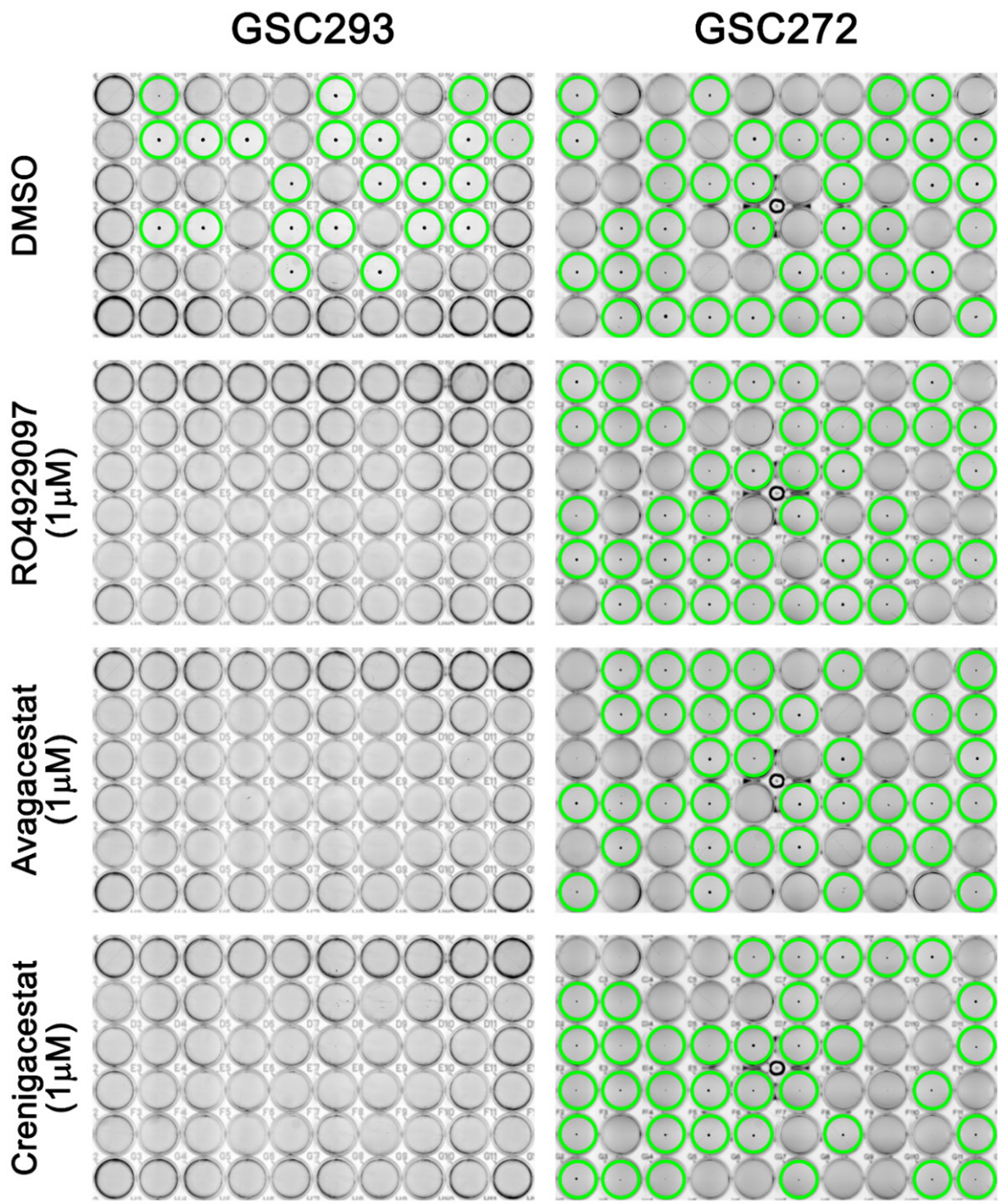


**Figure S1.** Representative images of GSC sphere formation after GSIs treatment. RO4929097, avagacestat, and crenigacestat treatment significantly attenuated sphere formation ability in GSC293 (wt-p53) but not in GSC272 (mut-p53). Wells with spheres were labeled by green circle. n = 3.

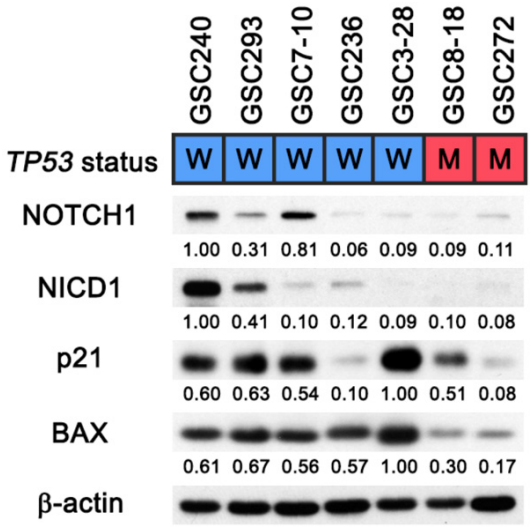


**Figure S2.** Expression of NOTCH1 signaling and p53 target genes in the validation group. The basal expression of NOTCH1 signaling (NOTCH1 and NICD1) and p53 target genes (p21 and BAX) was detected by Western blot analysis. *TP53* status (W: wild-type, M: mutant) is also shown. n = 3.

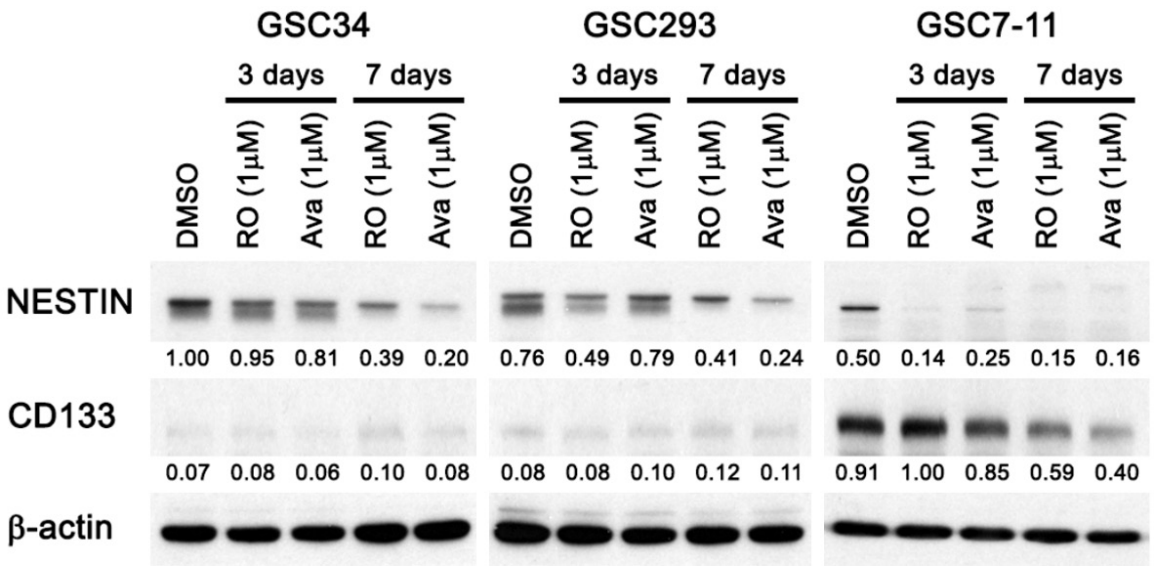


**Figure S3.** GSIs downregulated the expression of stem cell markers in GSCs. GSCs were treated by RO4929097 and avagacestat for 3 and 7 days. Both GSIs treatment decreased NESTIN and CD133 expression in GSCs. n = 3.

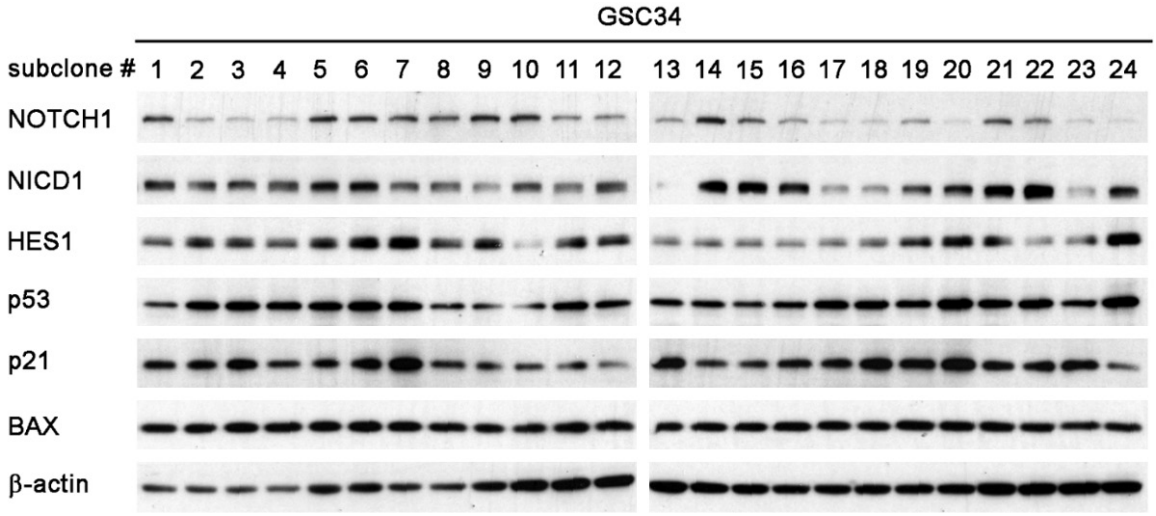


**Figure S4.** Expression of NOTCH1 and wt-p53 signaling in single cell-derived subclones of GSC34. Single cells from GSC34 were obtained by flowcytometry sorting. The single cell-derived subclones showed heterogenous expression pattern of NOTCH1 signaling and comparable wt-p53 activity.

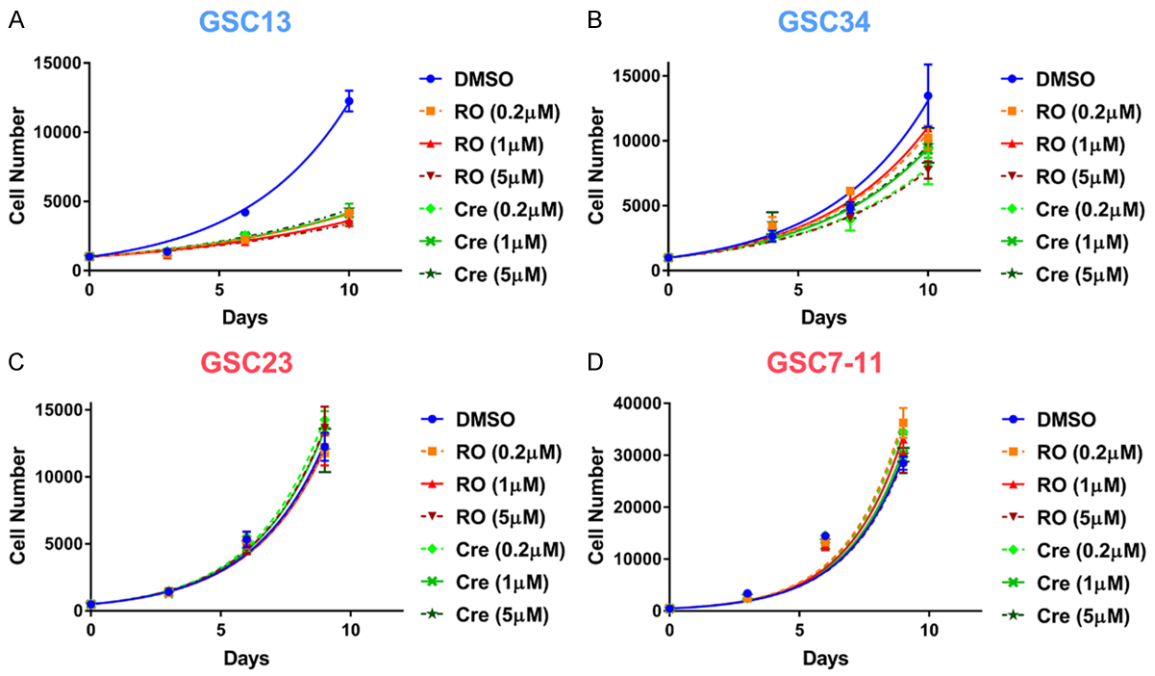


**Figure S5.** Effect of GSIs on GSC growth. The effect of GSIs (RO and crenigacestat) on GSC growth was tested in three doses (0.2 mM, 1 mM, and 5 mM). A, B. GSIs inhibited GSC13 (wt-p53) growth, but the effect was minimal in GSC34 (wt-p53). C, D. GSIs did not affect growth in mut-p53 GSCs (GSC23 and GSC7-11). n = 3. Blue font: wt-p53 cells. Red font: mut-p53 cells.

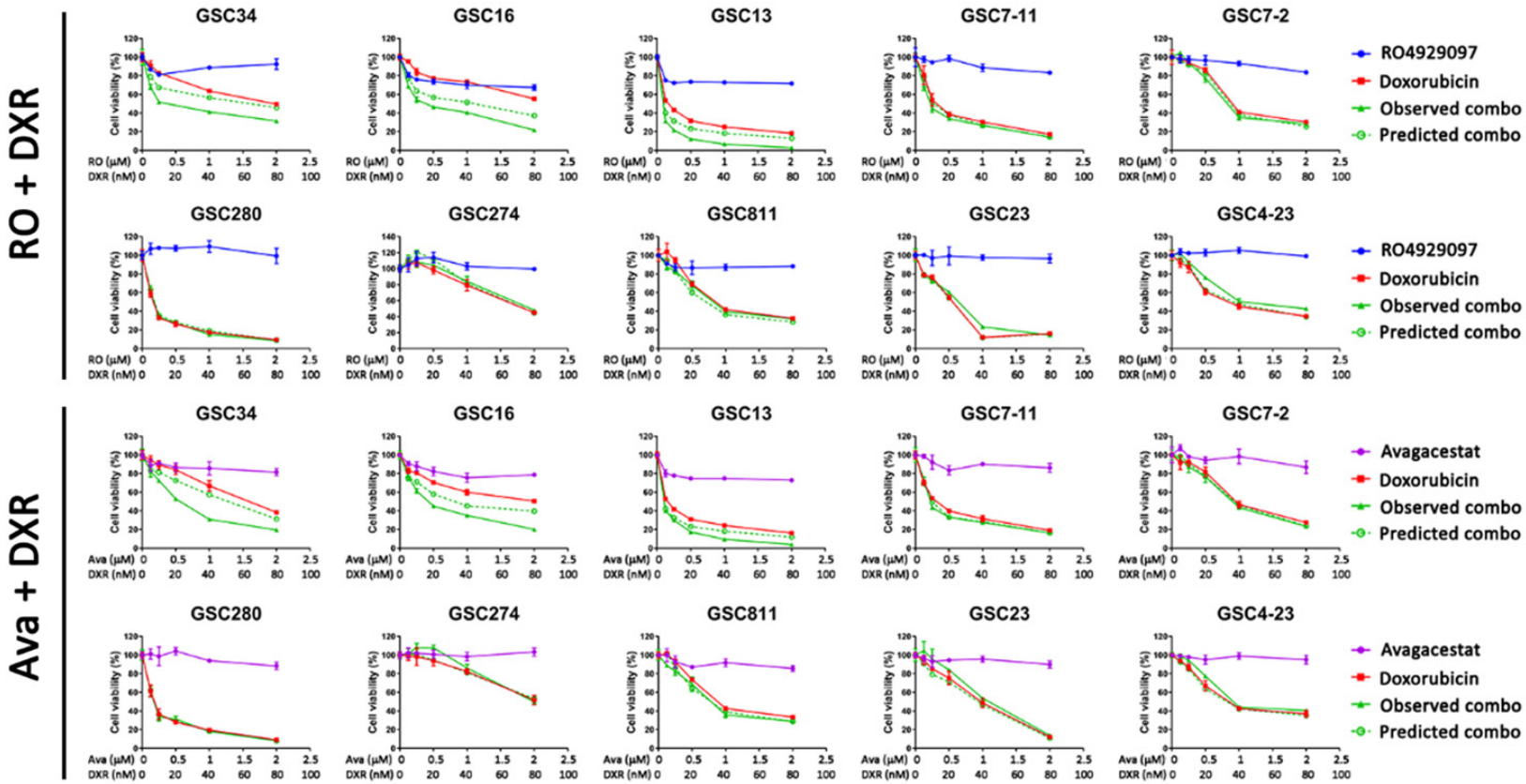


**Figure S6.** Screening group. The effect of GSI (RO or avagacestat) and doxorubicin treatment (5 days) on GSC proliferation. n = 3.

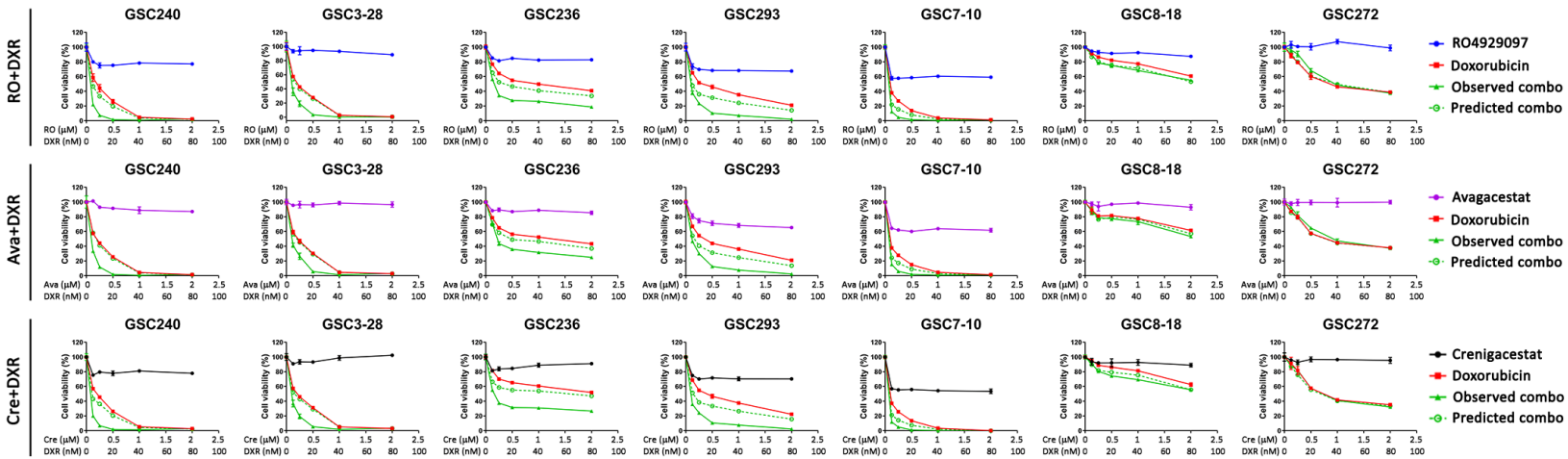


**Figure S7.** Validation group. The effect of GSI (RO, avagacestat, or crenigacestat) and doxorubicin treatment (5 days) on GSC proliferation. n = 3.

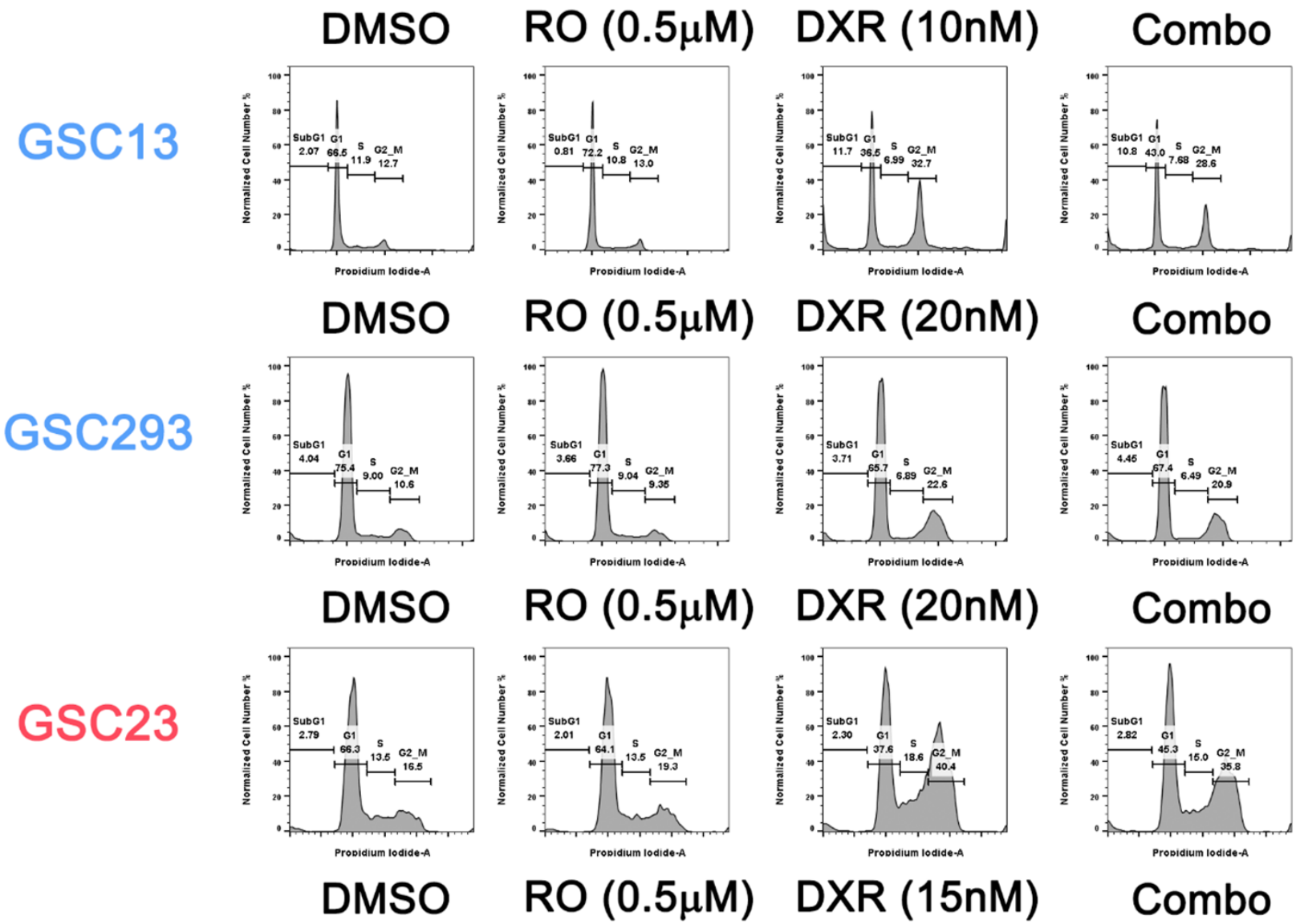
GSC13
DMSO
SubG1 2.07
G1 66.5
S 11.9
G2_M 12.7
RO (0.5μM)
SubG1 0.81
G1 72.2
S 10.8
G2_M 13.0
DXR (10nM)
SubG1 11.7
G1 36.5
S 6.99
G2_M 32.7
Combo
SubG1 10.8
G1 43.0
S 7.68
G2_M 28.6
GSC293
DMSO
SubG1 4.04
G1 75.4
S 9.00
G2_M 10.6
RO (0.5μM)
SubG1 3.66
G1 77.3
S 9.04
G2_M 9.35
DXR (20nM)
SubG1 3.71
G1 65.7
S 6.89
G2_M 22.6
Combo
SubG1 4.45
G1 67.4
S 6.49
G2_M 20.9
GSC23
DMSO
SubG1 2.79
G1 66.3
S 13.5
G2_M 16.5
RO (0.5μM)
SubG1 2.01
G1 64.1
S 13.5
G2_M 19.3
DXR (20nM)
SubG1 2.30
G1 37.6
S 18.6
G2_M 40.4
Combo
SubG1 2.82
G1 45.3
S 15.0
G2_M 35.8
DMSO
RO (0.5μM)
DXR (15nM)
Combo
Normalized Cell Number %
Propidium Iodide-A

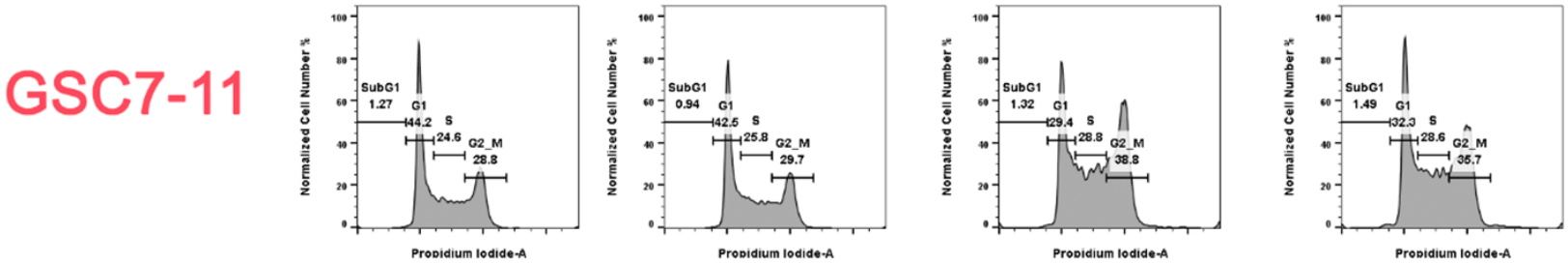


**Figure S8.** GSI and doxorubicin combination did not induce additional cell cycle arrest. GSCs were treated for 24 hours. Doxorubicin alone induced G2/M arrest in all four GSCs, while RO treatment did not facilitate doxorubicin to induce more cell cycle arrest. Doxorubicin concentration for apoptosis detection was determined by IC50 for each GSC. n = 3. Blue font: wt-p53 cells. Red font: mut-p53 cells.

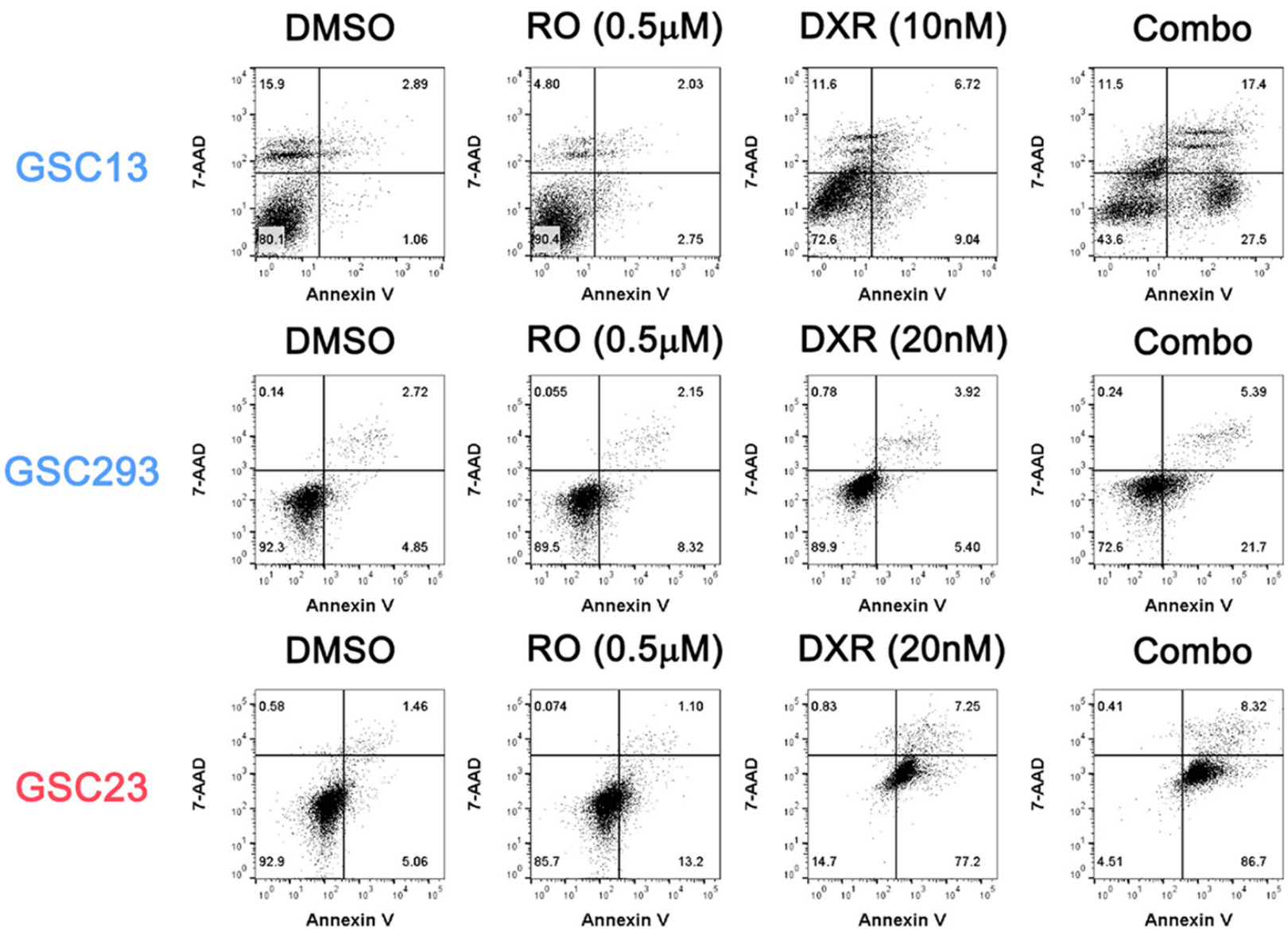
GSC13
GSC293
GSC23
DMSO
RO (0.5μM)
DXR (10nM)
DXR (20nM)
Combo
7-AAD
Annexin V
15.9
2.89
80.1
1.06
4.80
2.03
90.4
2.75
11.6
6.72
72.6
9.04
11.5
17.4
43.6
27.5
0.14
2.72
92.3
4.85
0.055
2.15
89.5
8.32
0.78
3.92
89.9
5.40
0.24
5.39
72.6
21.7
0.58
1.46
92.9
5.06
0.074
1.10
85.7
13.2
0.83
7.25
14.7
77.2
0.41
8.32
4.51
86.7

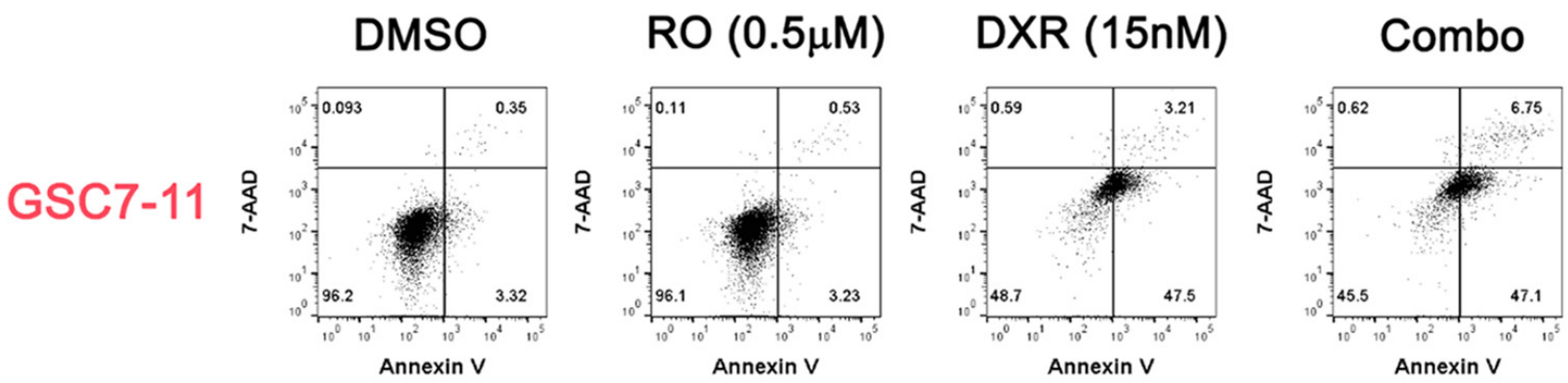


**Figure S9.** GSI and doxorubicin combination induced more apoptosis in wt-p53 GSCs. GSCs were treated for 24 hours and then stained with FITC-annexin V/7-AAD. Doxorubicin concentration for apoptosis detection was determined by IC50 for each GSC. n = 3. Blue font: wt-p53 cells. Red font: mut-p53 cells.

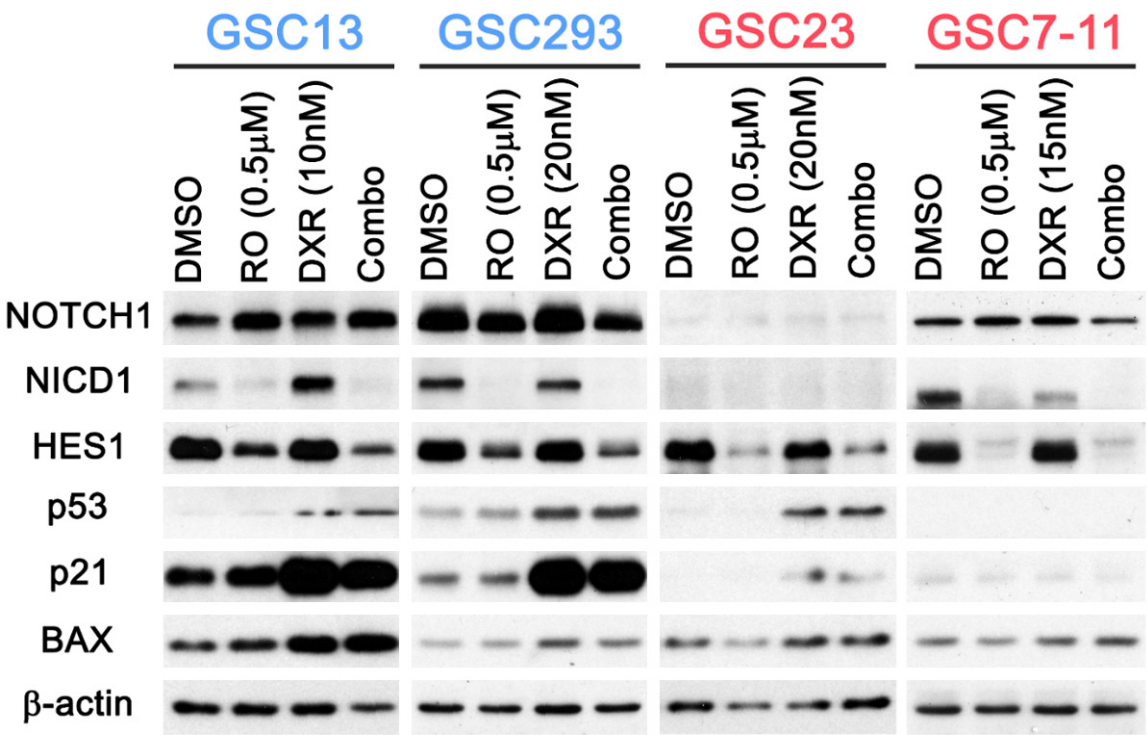


**Figure S10.** Effect of GSI and doxorubicin combination on NOTCH1 and p53 pathway expression. GSCs were treated for 24 hours and then subjected to Western blot analysis. Doxorubicin concentration for apoptosis detection was determined by IC50 for each GSC. n = 3. Blue font: wt-p53 cells. Red font: mut-p53 cells.